

This article was downloaded by: [Xian Jiaotong University]

On: 11 December 2014, At: 13:23

Publisher: Taylor & Francis

Informa Ltd Registered in England and Wales Registered Number: 1072954 Registered office: Mortimer House, 37-41 Mortimer Street, London W1T 3JH, UK



Molecular Crystals and Liquid Crystals

Publication details, including instructions for authors and subscription information:

<http://www.tandfonline.com/loi/gmcl20>

Birefringence Study in Hydrogen Bonded Complexes

C. Kavitha^a, N. Pongali Sathya Prabu^a & M. L. N. Madhu Mohan^a

^a Liquid Crystal Research Laboratory (LCRL), Bannari Amman

Institute of Technology, Sathyamangalam, 638 401, India

Published online: 28 Apr 2014.

To cite this article: C. Kavitha, N. Pongali Sathya Prabu & M. L. N. Madhu Mohan (2014) Birefringence Study in Hydrogen Bonded Complexes, *Molecular Crystals and Liquid Crystals*, 592:1, 163-180, DOI: [10.1080/15421406.2013.858012](https://doi.org/10.1080/15421406.2013.858012)

To link to this article: <http://dx.doi.org/10.1080/15421406.2013.858012>

PLEASE SCROLL DOWN FOR ARTICLE

Taylor & Francis makes every effort to ensure the accuracy of all the information (the "Content") contained in the publications on our platform. However, Taylor & Francis, our agents, and our licensors make no representations or warranties whatsoever as to the accuracy, completeness, or suitability for any purpose of the Content. Any opinions and views expressed in this publication are the opinions and views of the authors, and are not the views of or endorsed by Taylor & Francis. The accuracy of the Content should not be relied upon and should be independently verified with primary sources of information. Taylor and Francis shall not be liable for any losses, actions, claims, proceedings, demands, costs, expenses, damages, and other liabilities whatsoever or howsoever caused arising directly or indirectly in connection with, in relation to or arising out of the use of the Content.

This article may be used for research, teaching, and private study purposes. Any substantial or systematic reproduction, redistribution, reselling, loan, sub-licensing, systematic supply, or distribution in any form to anyone is expressly forbidden. Terms & Conditions of access and use can be found at <http://www.tandfonline.com/page/terms-and-conditions>

Birefringence Study in Hydrogen Bonded Complexes

C. KAVITHA, N. PONGALI SATHYA PRABU,
AND M. L. N. MADHU MOHAN*

Liquid Crystal Research Laboratory (LCRL), Bannari Amman Institute
of Technology, Sathyamangalam 638 401, India

A novel series of linear complementary hydrogen bonded complexes fashioned between p-n-alkylbenzoic acids (nBA) and m-fluorobenzoic acid (FBA) are isolated. The obtained homologous series comprising of seven mesogens are analyzed by polarizing optical microscope (POM), differential scanning calorimetry (DSC) and Fourier Transform Infra-Red (FTIR) spectroscopy. It is interesting to note the correlation between the alkyl chain length and the mesogenic phases. The order of the transitions is examined through Cox parameter, experimentally derived by thermal analysis (DSC). Optical tilt angle studies in smectic C and thermal stability factors for various phases are discussed. Birefringence study by various techniques enabled to measure the refractive index at various phase transitions. These results are compared and conferred with those obtained from conventional refractometer. Further orientational order parameter for various phases has been discussed.

Keywords Cox parameter; hydrogen bonding; m-fluorobenzoic acid; order parameter

1. Introduction

Hydrogen bonding is one of the important interactions in nature [1]. Hydrogen bonds range from the very strong covalent bonds, to the very weak Vander Waals forces. Most hydrogen bonds are weak attractions with a binding strength of about one-tenth of that of a normal covalent bond. Liquid crystals formed by hydrogen bonds are molecular materials that coalesce anisotropy with dynamic nature in which, stimulation and stabilization of liquid crystallinity through such hydrogen bonds are now well-established. Among various aspects, the shape and size of the molecular constituents and a delicate balance of non-covalent intermolecular interactions govern the phase behavior of liquid crystals [1,2].

In recent times [3], the use of hydrogen bonding for the design and synthesis of functional liquid crystalline materials has been shown to be a versatile approach towards the control of simple molecularly self-assembled structures and the induction of dynamic function. The existence of mesophases has been favored in several liquid crystals through self-complementary intermolecular hydrogen bonding [3–6].

Lehn and coworkers [7,8] used different complementary molecules to form Supramolecular Hydrogen Bonded Liquid Crystals (SMHBLC). Simple hydrogen bonded systems with carboxylic acids or phenols as proton donors and pyridyl groups as proton

*Address correspondence to M. L. N. Madhu Mohan, Liquid Crystal Research Laboratory (LCRL), Bannari Amman Institute of Technology, Sathyamangalam 638 401, India. Tel: +91 9442437480; Fax: +91 4295 223 775. E-mail: lakshminarayanammohan@bitsathy.ac.in

acceptors have been studied extensively by the research groups of Kato, Frechet, Bruce, and Yu [9–14]. Hydrogen bonding is a powerful tool for stabilizing and inducing mesophases, even in compounds where the structure largely deviates from that of the classical calamitic liquid crystals [15].

The role of hydrogen bonding interactions in the formation and/or stabilization of liquid crystalline phases have been recognized in recent years and significant work has been conducted. Following the first and well-established examples of liquid crystal formation through the dimerization of aromatic carboxylic acids, several classes of compounds have been prepared [16]. By the interaction of complementary molecules, the liquid crystalline behavior is crucially dependent on the structure of the resulting supramolecular systems. Depending on the nature, number, and position of the groups able to form hydrogen bonds, a diversity of supramolecular structures, both dimeric and polymeric, have been obtained [17], affording in turn various liquid crystalline phases.

Liquid crystals fascinated attention during the last decade and the references there in [18–24]. Molecular interactions received significant influence on the ordering of liquid crystalline state. A powerful tool towards designing of highly organized soft matter arises from strong cohesive forces such as hydrogen bonding between identical or complementary molecules [25,26]. A number of such systems have been investigated, following the reports of Kato and Frechet Jean [27–33] and are reviewed extensively [3,34]. A wide variety of self-organized molecular systems, such as liquid crystals attracted to produce functional materials [35]. Shandryuk [36] studied the orientation behavior of liquid crystal networks stabilized by hydrogen bonds. This type of interaction possesses utility in the area of miscibility of liquid crystalline blends and in the design of novel guest–host liquid crystalline systems as well. Thus the present investigation focuses on the self-assembled liquid crystals generated through inter-molecular hydrogen bonding.

It is well known, [1] that liquid crystals are anisotropic in nature and hence are found to be birefringent. Light polarized parallel to the director has a different index of refraction than light polarized perpendicular to the director. As a consequence, when light enters a birefringent material, such as a nematic liquid crystal, the process is modeled in terms of the light being broken up into the fast ordinary ray (n_o) and the slow extraordinary ray (n_e) components. Since the two components travel at diverse velocities, the waves get out of phase. When the rays are recombined as they exit the birefringent material, the polarization state has changed because of this phase difference. The birefringence of a material (Δn) is characterized by the difference of n_e and n_o . For typical nematic liquid crystals, n_o is approximately 1.5 and the maximum difference Δn , may range between 0.05 and 0.5. In the present investigation, order parameter of the liquid crystal in various phases is studied.

2. Experimental

Optical textural observations were made with Nikon polarizing microscope equipped with Nikon digital Charge-Coupled Device (CCD) camera system with 5 mega pixels and 2560×1920 pixel resolutions. Liquid crystalline textures were stored, retrieved, and analyzed with the aid of NIS element version 4 imaging advanced software. Temperature control of the liquid crystal cell was equipped by Instec HCS402-STC 200 temperature controller (Instec, USA) to a temperature resolution of $\pm 0.1^\circ\text{C}$. This unit was further interfaced to a computer by IEEE –STC 200 to control and monitor the temperature. Liquid crystal sample was filled by capillary action in its isotropic state into a commercially available (Instec, USA) polyamide buffed cell with $4\ \mu\text{m}$ spacer. Optical extinction technique [37–39] was used for

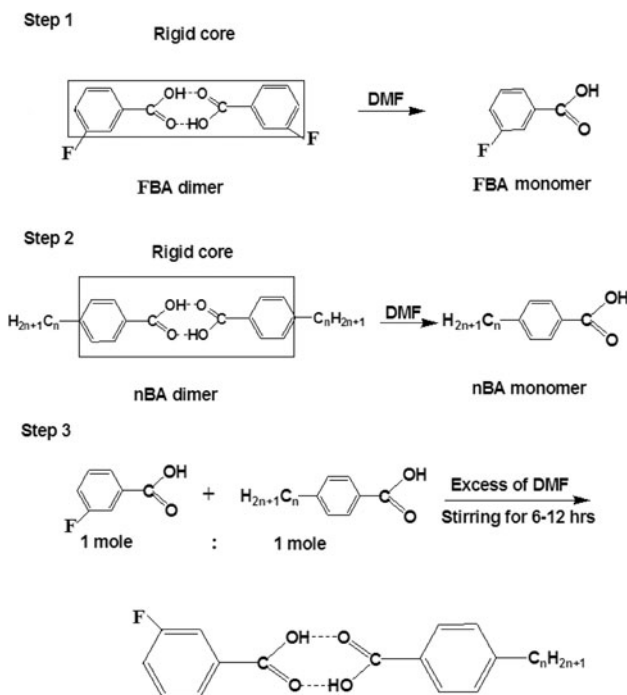


Figure 1. Synthesis scheme representing the formation of FBA + *n*BA hydrogen bonded series along with its molecular design.

the determination of tilt angle. Transition temperatures and corresponding enthalpy values were experimentally deduced by DSC (Shimadzu DSC-60, Kyoto, Japan). Fourier transform infra-red (FTIR) spectra was recorded (ABB FTIR MB3000, Quebec, Canada) and analyzed with the MB3000 software. Refractive index measurements were made with the assist of refractometer (Abbe 5, Kent, UK). The *m*-fluorobenzoic acid (FBA) and *p*-*n*-alkyl benzoic acids (*n*BA, where $m = 2-8$) were supplied by Sigma Aldrich, (Steinheim, Germany) and all the solvents were of High-Performance Liquid Chromatography (HPLC) grade.

3. Synthesis

All the intermolecular hydrogen bonded complexes examined in the present study are obtained by mixing equimolar ratios of FBA with various *n*BA in excess DMF and reprecipitating after the evaporation of excess solvent as reported in literature [40] and the series is referred as FBA + *n*BA. Synthetic route and molecular structure of the present HBLCs are designed with *m*-fluorobenzoic acid and various *p*-*n*-alkylbenzoic acids (FBA + *n*BA, where $n = 2-8$) and the molecular structure along with the scheme is presented in Fig. 1.

4. Results and Discussion

FBA + *n*BA intermolecular hydrogen bonded complexes isolated under the present investigation are white crystalline solids and are stable at room temperature (30°C). They are insoluble in water and sparingly soluble in common organic solvents, such as methanol, ethanol, benzene, and dichloro methane. However, they show a high degree of solubility in

Table 1. Transition temperatures and enthalpy values obtained by various techniques for FBA + *n*BA homologous series

Complex	Phase variance	Technique	Melt	<i>N</i>	<i>C</i>	<i>F</i>	Crystal
FBA + 8BA	NCF	DSC(h)	68.61 (13.21)	@ 84.2 (1.04)	83.5 (10.56)	@	49.4 (13.20) 49.5
		DSC(c)			76.6 (8.97)	#	
		POM(c)			77.1	63.4	
FBA + 7BA	NCF	DSC(h)	66.6 (45.26)	@ 71.4 (0.86)	@	*	53.0 (41.89) 53.1
		DSC(c)			65.6 (0.94)	*	
		POM(c)			65.8	54.7	
FBA + 6BA	CF	DSC(h)	63.4 (37.95)	@ 61.7 (0.98)	@	*	51.3 (36.2) 51.4
		DSC(c)			61.9	*	
		POM(c)			66.4 (1.37)	53.7	
FBA + 5BA	CF	DSC(h)	58.1 (25.03)	@ 58.0 (0.53)	58.2	@	45.4 (22.79) 45.5
		DSC(c)			51.2 (0.26)	51.4 (2.47)	
		POM(c)			51.5	51.5	
FBA + 4BA	CF	DSC(h)	65.5 (44.68)	@ 65.1 (31.91)	@	@	47.5 (36.14) 47.6
		DSC(c)			51.6	#	
		POM(c)			61.8 (3.22)	49.5	
FBA + 3BA	F	DSC(h)	86.2 (44.33)	@ 90.2 (4.80)	62.0	@	51.0 (27.62) 51.1
		DSC(c)			90.4	66.8 (23.21)	
		POM(c)			66.9	66.9	

Temperatures in °C, Enthalpy J/g is given in parenthesis, * not resolved, @ monotropic transition, #Merged with crystal, (h) heating run, (c) cooling run.

coordinating solvents like dimethyl sulfoxide (DMSO), dimethyl formamide (DMF), and pyridine. They melt at temperatures below 58.0°C (Table 1) and show high thermal and chemical stability when subjected to repeated thermal scans performed during polarizing optical microscopy (POM) and differential scanning calorimetry (DSC) studies.

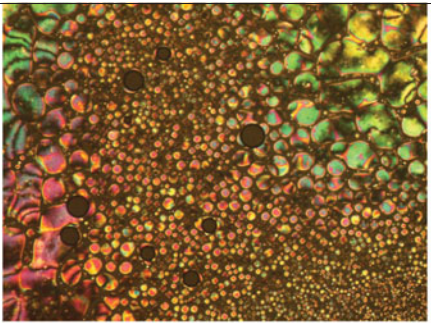

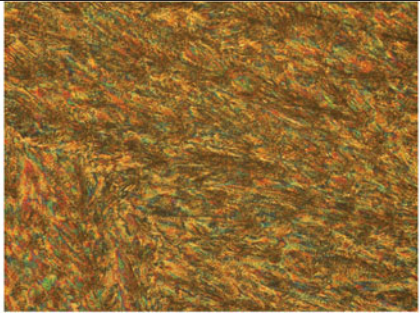
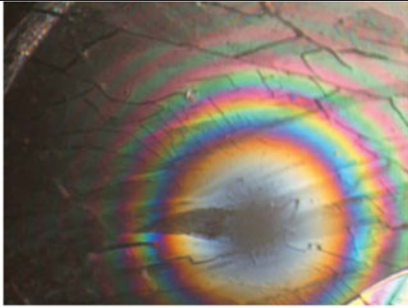
4.1. Phase Identification

Phase variance, transition temperatures, and the corresponding enthalpy values obtained in the cooling and heating cycles of DSC and cooling studies of POM for the FBA + n BA complexes are presented in Table 1. The series exhibit rich phase variance with nematic, smectic C , and smectic F phases. Phase transition from smectic C to smectic F in all the mesogens during the cooling run is observed to be monotropic.

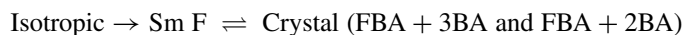
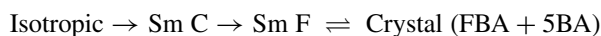
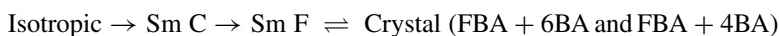
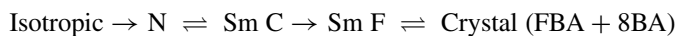
4.2. Mesogenic Nature of FBA + n BA

Liquid crystalline complexes of the FBA with n BA (where $n = 2-8$) designated as FBA + n BA homologous series, are found to exhibit characteristic textures, [35], viz., nematic (droplets, Plate 1), smectic C (schlieren texture, Plate 2), and smectic F (mosaic-schlieren Plate 3, i.e., mosaic platelets separated by very fine lines). General phase sequence of the

PLATES

	
<p>Plate 1. Droplet texture of nematic phase.</p>	<p>Plate 2. Schlieren texture of smectic C phase.</p>
	
<p>Plate 3. Mosaic-schlieren texture of smectic F phase.</p>	<p>Plate 4. Newton rings pattern of FBA + 7BA at 67°C obtained by polychromatic source.</p>

various homologues of FBA + *n*BA series in cooling and heating runs can be shown as:



Monotropic and enantiotropic transitions are depicted as single and double arrows, respectively.

4.3. Fourier Transform Infrared Spectroscopy (FTIR)

FTIR spectra of all the HBLC complexes are recorded in the solid state (KBr) at room temperature (30°C). As a representative case, Fig. 2 illustrates the FTIR spectra of FBA + 7BA in solid state at room temperature that is discussed elaborately. It is reported [41,42] that in alkylbenzoic acids, if carboxylic acid exists in monomeric form, the stretching vibration of C=O is observed at 1760 cm⁻¹. Further, it is reported [42] that when a hydrogen bond is formed between carboxylic acids, it results in lowering of the carbonyl frequency, which has been noticed in the present hydrogen bonded complexes. A noteworthy feature in the spectrum of the FBA + 7BA complex is the appearance of sharp peak at 1693 cm⁻¹ that clearly implies the dimer formation [42–46] and 2922 cm⁻¹ for OH stretching frequency for hydrogen bonded complexes. A carboxylic acid existing in monomeric form in dilute solution absorbs at about 1760 cm⁻¹ owing to the electron withdrawing effect [42]. However, acids in concentration solution or in solid state have a tendency to dimerize through hydrogen bonding. It is reported [42] that this dimerization weakens the C=O bond there by lowering the stretching force constant *K*, resulting in a lowering of the carbonyl frequency of saturated acids to 1693 cm⁻¹. Hence, in the synthesized complexes, the formation of hydrogen bonding is established by FTIR, which clearly depicts a similar trend of result in all the hydrogen bonded complexes of the series.

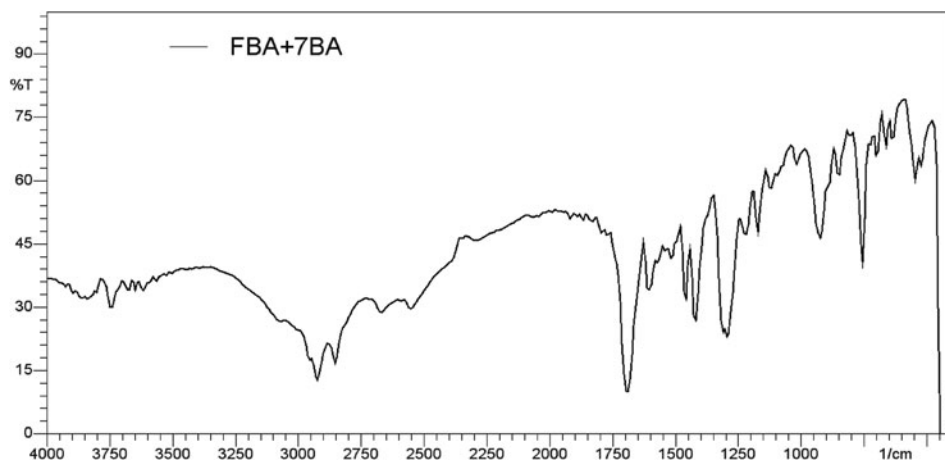


Figure 2. FTIR spectra of FBA + 7BA complex.

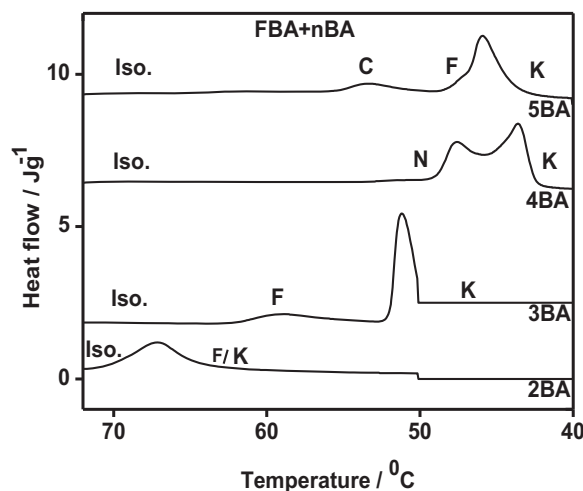


Figure 3. DSC thermogram of FBA + n BA ($n = 2-5$) complex.

4.4. Differential Scanning Calorimetry (DSC)

DSC thermograms are recorded both in heating and cooling cycle. The empty aluminium pan is weighed initially and the desired mesogen of a predetermined weight is filled in it before crimping. The crimped aluminium pan along with the sample is placed in the heating chamber of DSC where another crimped empty aluminium pan is taken as the reference. In the heating chamber, nitrogen gas is purged at a constant rate in order to facilitate a continuous flow of gas and to maintain an inert atmosphere. DSC thermograms are recorded, stored, and analyzed by TA60 data software. The mesogen is heated with a scan rate of $10^{\circ}\text{C}/\text{min}$ and held at its isotropic temperature for 2 min so as to attain thermal stability and the cooling run is performed with the same scan rate. The same is repeated with $5^{\circ}\text{C}/\text{min}$ scan rate also. Experimentally obtained equilibrium transition temperatures and the corresponding enthalpy values of the mesogens are listed separately in Table 1 and the representative thermograms of various mesogens are depicted in Fig. 3. It can be noticed that the transition temperatures obtained by POM studies reasonably synchronize with the data obtained from DSC studies.

4.5. Phase Diagram

Phase diagram of the present homologous series is constructed with POM and DSC data and is illustrated as Fig. 4. The following are the points that can be drawn from the phase diagram.

- i) Phase diagram is comprised of nematic phase and two smectic phases viz., smectic C and smectic F .
- ii) Nematic phase is found prevalent only in higher homologues and is quenched completely in the lower counter parts.
- iii) Smectic F phase is observed in all the mesogens while nematic and smectic C phases are observed in higher homologues from heptyl and butyl carbon numbers, respectively.

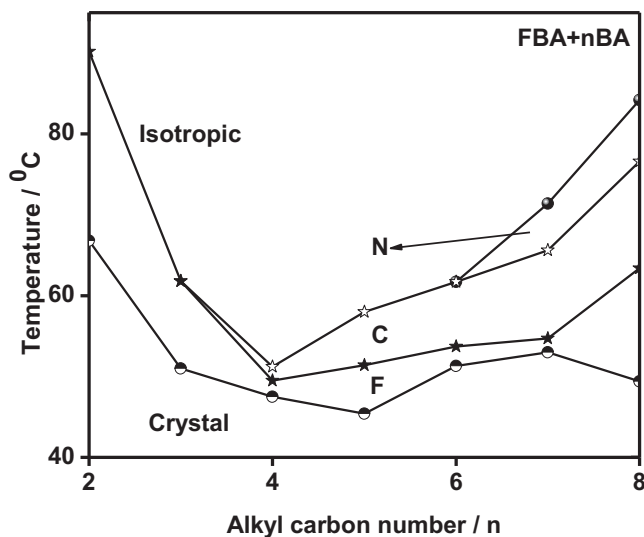


Figure 4. Phase diagram of FBA + n BA homologous series.

- iv) All the complexes possess a wide thermal span of the mesogenic phases and the mesogenic thermal range of the liquid crystals is separately depicted in Fig. 5.
- v) Fig. 5 clearly depicts that the mesogenic thermal range is highly influenced by the alkyl carbon chain length and further, the odd and the even alkyl chain has different trends.
- vi) Both the higher and the lower homologues of the series possess higher mesogenic thermal range compared to the intermediate ones.

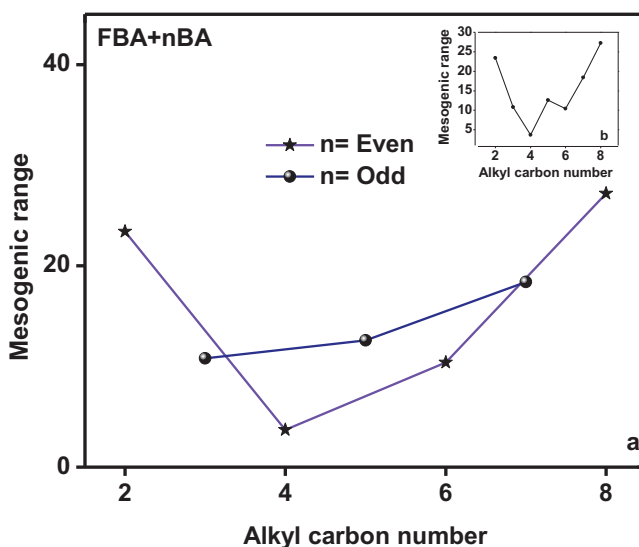


Figure 5. Mesogenic thermal ranges for the FBA + n BA homologues.

- vii) Higher ordered smectic *F* phase is observed in all the complexes of the entire series.

4.6. Thermal Analysis

From the thorough observation of the DSC thermograms, it is not surprising to note that in all the mesogens under investigation, the magnitude of the sum of individual enthalpy values obtained by the various phase are found to be identical in the cooling and the heating run, respectively. As a representative case, in FBA + 7BA the sum of the enthalpy value of the transitions, i.e., from isotropic to nematic, nematic to smectic *C*, smectic *C* to smectic *F*, and smectic *F* to crystal are found to be identical in the heating and the cooling runs of DSC. In Table 2 the corresponding enthalpy values in heating and cooling run of DSC of individual phases are compiled and the sum of enthalpy values in cooling and heating run are found to be almost identical. Hence, the thermal energy of the system is conserved as per the laws of thermodynamics.

4.6.1. Cox Parameter. Landau theory and Mean field theory [1,47,48] are the theories that discuss the phase transitions in liquid crystalline substance. These two theories on the whole can be summarized as, a physical system in which phase transition can occur is usually characterized by one or more long range order parameters. A phase transition can be accompanied either by a continuous change or by a discontinuous change in the equilibrium value of the order parameter when the system transforms from one phase to the other. It is said to be the first order transition when it is discontinuous and if the state is continuous it is assigned to be second order transition. Thus, the theoretical description of a phase transition is equivalent to the determination of the free energy density as a function of the order parameter, its spatial derivatives and the temperature. Determination of order of the phase transition by experimental technique carried out by Navard and Cox [49] supplements the above mentioned arguments.

Navard and Cox [49] executed a new experimental method in determining the order of transition, where the scan rate of the sample or the weight of the sample can be a varying parameter with respect to the phase transition peak height obtained by DSC thermograms. In this present work the variation in scan rate namely 5°C/min and 10°C/min has been considered for practical convenience. According to Cox theory, the first and second order

Table 2. Sum of enthalpy values obtained in heating and cooling run for FBA + *n*BA homologous series

Complex	ΣEnthalpy in DSC cycles	
	Endothermic cycle (J/g)	Exothermic cycle (J/g)
FBA + 8BA	23.77	23.72
FBA + 7BA	45.26	44.42
FBA + 6BA	37.95	37.18
FBA + 5BA	26.4	25.79
FBA + 4BA	44.68	36.40
FBA + 3BA	31.91	30.84

Table 3. Comparison of DSC peak heights along with N_C values across various transitions in FBA + n BA complexes

Complex	Phase	N_C Ratio	Order of transition
FBA + 8BA	C	1.44	First
FBA + 7BA	C	2.17	Second
FBA + 5BA	C	2	Second
	F	1.05	First
FBA + 4BA	F	1.54	First
FBA + 3BA	F	1.0	First
FBA + 2BA	F	1.41	First

transitions can be classified basing on the ratio (N_C) of the measured phase transition peak heights. The ratio (N_C) is $1 < N_C \leq \sqrt{2}$ for an isothermal first order transition and $N_C = 2$ for a second order transition.

For all the homologues, DSC thermograms at 5°C/min and 10°C/min are obtained and the thermal analysis of the entire homologues series is discussed. The values of N_C for the smectic C and smectic F transitions for all the complexes are presented in Table 3. From this qualitative analysis the value of N_C is found to be below 2 indicating that all smectic F transitions are of first order, whereas smectic C phase transition is either first or second order transitions. Quantitatively, the higher magnitude of enthalpy obtained in DSC studies (Table 1) also serves as an additional evidence for its first order transition.

4.6.2. Thermal Stability Factor. The term thermal stability can be attributed to the transition temperature as well as to the temperature range of a particular phase. Hence it is highly important to consider both the factors and define a parameter called the stability factor, S [50] and it is defined as:

$$S = T_{\text{mid}} * \Delta T_{\text{phase}},$$

where T_{mid} is the mid-temperature of the phase and ΔT_{phase} , the temperature range of the particular phase.

Table 4. Thermal stability factor correlation for smectic C and smectic F phases

Complex	Thermal stability factor	
	C	F
FBA + 8BA	4702.5	4579.3
FBA + 7BA	3699.1	523.0
FBA + 6BA	2712.6	748.8
FBA + 5BA	2196.6	1929.0
FBA + 4BA	679.4	610.9
FBA + 3BA	—	3592.1
FBA + 2BA	—	8263.8

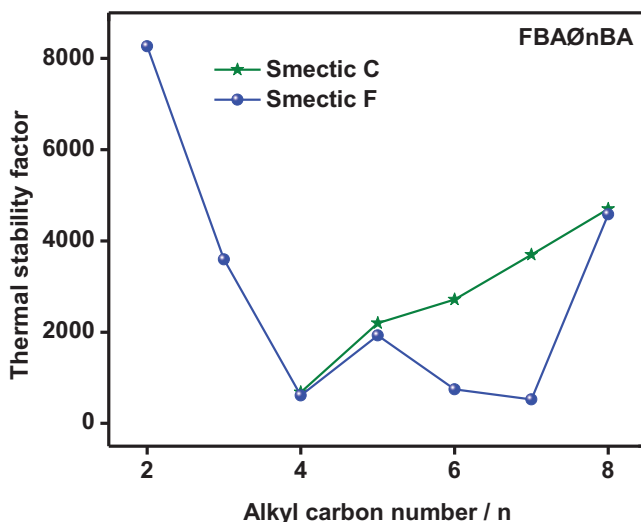


Figure 6. Thermal stability factors for smectic *C* and smectic *F* phases of FBA + *n*BA series.

From Figure 6 and Table 4, it is evident that the thermal stability of the smectic *C* phase shows a steady increase with the increase in alkyl chain length and this may be attributed to the increase in the electron donating nature of alkyl group (+I effect), whereas smectic *F* phase has varied effect.

4.7. Optical Tilt Angle Studies

Smectic *C* phase is the tilted smectic phase, where their molecular long axes of the constituent molecules are tilted with respect to normal to the layer planes [1]. The occurrence of the smectic *C* phase and the dependence of which upon the molecular structure and the temperature has been thoroughly verified by numerous experimental studies. The conclusions and the findings from these results suits best for the present series (FBA + *n*BA) under investigation and they can be concluded as:

- i) Smectic *C* phase is very well dependent upon the molecular structure of the constituent molecules, that too on the length of the carbon chain and the alkyl terminal groups.
- ii) Smectic *C* phase existing in the series depends on the structures having two terminal groups viz., alkyl groups attached to the rigid core of benzene.
- iii) Symmetrical molecular structures (benzoic acids) also favor the growth of smectic *C* phase in the homologous series.

As the smectic *C* phase depends upon the temperature, the optical tilt angle has been experimentally measured by optical extinction method [37] in smectic *C* phase of all the members of the present FBA + *n*BA homologous series exhibiting smectic *C* phase. Figure 7 depicts such variation of optical tilt angle with temperature for FBA + 7BA as a representative case. In Fig. 7 the theoretical fit obtained is denoted by the solid line and the error bars are also drawn. Further, it can be observed that the tilt angle increases with decreasing temperature. For the complex FBA + 7BA, the highest magnitude of tilt angle is observed to be around $\sim 23^\circ$. These large magnitudes of the tilt angle are attributed to the

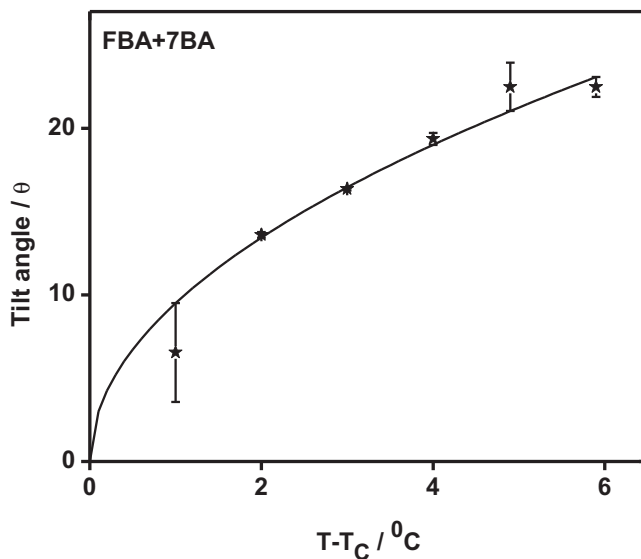


Figure 7. Temperature variation of tilt angle in smectic *C* phase of FBA + 7BA complex.

direction of the soft covalent hydrogen bond interaction which spreads along molecular long axis with finite inclination. Tilt angle is a primary order parameter [37] and the temperature variation is estimated by fitting the observed data of $\theta(T)$ to the relation

$$\theta(T) \propto (T_C - T)^\beta. \quad (1)$$

The critical exponent β value estimated by fitting the data of $\theta(T)$ to the above Equation (1) is found to be 0.50 to agree with the Mean field prediction [1,47,48]. Further, the agreement of magnitude of β (0.50) with Mean field predicted value (0.50) infers the long-range interaction of transverse dipole moment for the stabilization of tilted smectic *C* phase.

4.8. Method for the Determination of Order Parameter

A simple procedure is reported [51] for the determination of the order parameter (S) from the birefringence measurements, which can be applied for nematic and some smectic liquid crystal phases. In this technique, the birefringence δn is measured as a substitute for the measurement of two refractive indices (n_o , n_e) and density (d). Frequently used techniques include interference [52] and wedge technique [53], in these the distance between interference fringes in a wedge-shaped sample are measured. With the exception of many advantages, it has one drawback, i.e., complexity in the determination of the wedge angle with greater accuracy, as the wedge angle undergoes irreversible changes with time and temperature. For these reasons a slight modification of the wedge method has been reported [51] by Kuczyński et al. Different experimental methods are accessible for the determination of the order parameter in nematic liquid crystals. However, the same cannot be applicable and useful for the phases other than nematic. Thus, the extrapolation technique utilized by Kuczynski following the suggestion made by de Gennes viz., [54] that any anisotropic physical quantity may be a measure of orientational ordering in nematic mesophases has

been tracked. With this, the order parameter has been calculated based on birefringence measurements in this present work.

In the present investigation, a plane glass plate and a plane-convex lens of known curvature radius (R) are considered. This method is reported [50] for the refractometric measurements, i.e., with a further approximation effected by neglecting the internal polarization field to let order parameter, S be proportional to the observed birefringence. Thus the observed interference rings resulting from interference of light rays reflected on the surface of plate and lens measures both refractive indices separately. The radius of curvature ($R = 13.5$ mm) of the lens can be determined with the aid of Newton rings, which is very stable and does not change with temperature. Liquid crystal sample is introduced carefully into the air gap between lens and plate and the whole setup is placed between the crossed polarizer on a microscope stage. The liquid crystal sample is brought to its isotropic states thrice, in order to bring it to an even isotropic thermal equilibrium condition.

A system of concentric rings as shown in Plate 4 is visualized, which results from interference of the ordinary and the extraordinary rays after passing the analyzer. The sample alignment does not alter the formation of Newton rings. Further the rings are very distinct due to the crossed polarizer arrangement and the interference of transmitted rays rather than reflected rays.

The optical path difference of the ordinary and the extraordinary waves $y\delta n$ corresponding to a given bright ring is $k\lambda$ (y denotes the sample thickness in the middle of the ring, λ is the wavelength of light, and k is order of interference, i.e., the successive ring number). The thickness y can be calculated from the formula

$$y = x^2/2R,$$

where x denotes the radius of the considered ring and R is the radius of curvature of the plane-convex lens. Thus, the birefringence δn can be determined with a great accuracy (better than 10^{-3}) from the slope of the line representing the x^2 on k dependence. The same result can be obtained even if the dark rings are considered. The birefringence is measured as a function of temperature and is fitted as follows:

$$\delta n = \Delta n [1 - (T/T^*)]^\beta$$

where T is the absolute temperature, T^* and β are constants (T^* is about 1–4 K higher than the clearing temperature and the exponent β is close to 0.2). This procedure enables extrapolation of δn to the absolute zero temperature. In practice, values of three adjustable parameters T^* , Δn , and β were obtained by fitting the experimental data for δn to Equation written in the logarithmic form

$$\log \delta n = \log \Delta n + \beta \log [1 - (T/T^*)].$$

The values of $\log \Delta n$ and β can be calculated by the linear regression method and the parameter T^* was adjusted to get the best correlation coefficient of the linear regression. Thus, the order parameter, according to Equation is

$$S = \delta n / \Delta n.$$

The value of S determined in this way describes well the nematic order and is a good approximation of the order parameter S .

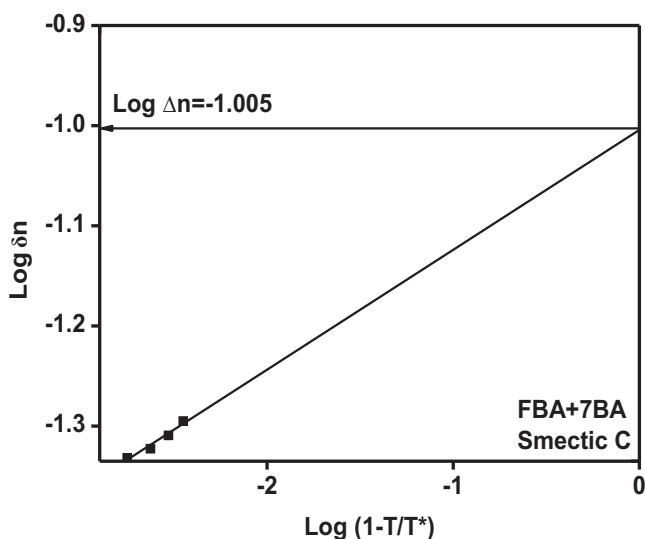


Figure 8. The log–log plot of birefringence (δn), against reduced temperature for the FBA + 7BA complex in smectic *C* phase.

Figures 8 and 9 indicate the variation of $\log \delta n$ with $\log (1-T/T^*)$ for the smectic *C* and smectic *F* phase, respectively. The $\log \Delta n$ value extrapolated for the crystal at 0 K from Figs. 8 and 9 are -1.005 and -0.875 , respectively, which on further evaluation yields 0.366 and 0.416 as the Δn value. The validity of δn extrapolation to determine Δn is in addition confirmed by the results of δn measurements performed in the solid state (Fig. 10), which is almost the same (approximately 0.33) as that of the extrapolated value. Further, the refractive index values have also been measured with the aid of Abbe 5 Refractometer

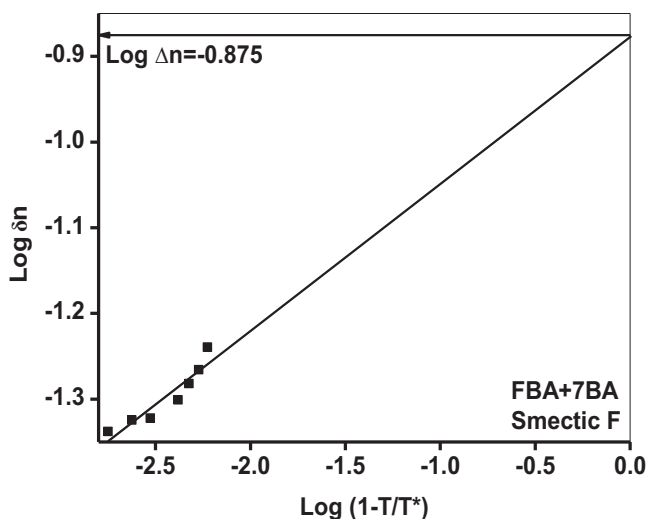


Figure 9. The log–log plot of birefringence (δn), against reduced temperature for the FBA + 7BA complex in smectic *F* phase.

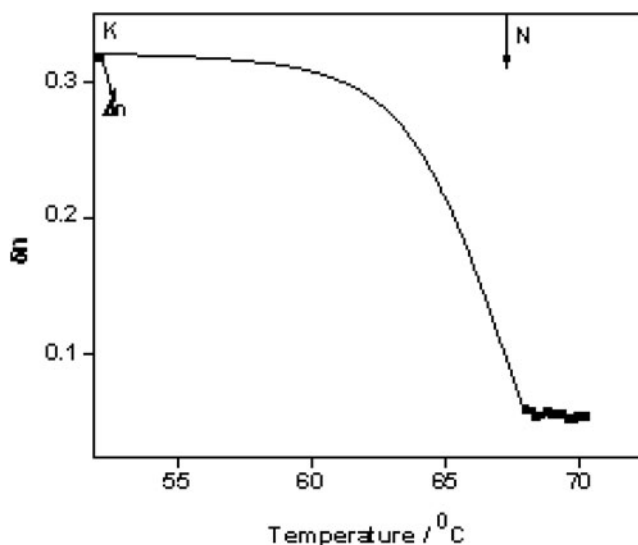


Figure 10. Temperature dependence of the birefringence (δn), for FBA + 7BA complex in the nematic (N) and crystalline (K) phases measured by the Newton rings method.

at various temperature ranges for all the obtained phases and are found to be in correlation with the data obtained by this method.

4.8.1. Comparison of the Order Parameter with Refractometer Studies. Abbe 5 Refractometer is ideally suited for use, where wide refractive index measurement range is required. The liquid crystal sample in its isotropic state is transferred to the lower prism using a pipette and the upper prism is closed, securing it with the locking knob. Care should be taken to cover evenly the prism surface with the liquid crystal sample, without any air bubbles. The sample is then illuminated by aligning the chrome-plated reflector with a suitable light source. Adjustment of achromatizing prisms by rotating the dispersion knob provides a means of ensuring that the reading is obtained at the correct wavelength. As the refractive index of a liquid varies with temperature, the instrument must be controlled at a fixed temperature by circulating water. Water bath connections provide prism temperature control, with the prism temperature being monitored electronically and displayed on the integral, battery powered, and digital display. The eyepiece is rotated to focus the scale and the borderline display and the dispersion knob is adjusted to remove color and create a sharp borderline, which aligns with the centre of the crosswire. With good temperature control and precise calibration, readings of refractive index may be obtained to four decimal places.

Figure 11 clearly indicates that the δn value when plotted against the temperature shows a constant slope for isotropic condition. Further the nematic phase exhibits a steep positive slope where as a negative slope is obtained for both smectic *C* and smectic *F*. The phase transitions from isotropic to nematic, nematic to smectic *C*, smectic *C* to smectic *F* are very well established from the Fig. 11, which is further confirmed from the values of order parameter as exhibited in Fig. 12. The order parameter value is maximum at the isotropic state and it goes on decreasing as the temperature is decremented towards attaining the crystal, which has the lowest order parameter of the order of 0.33.

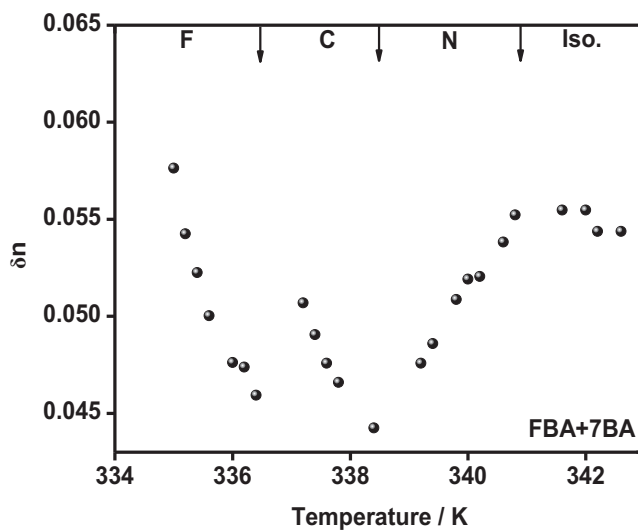


Figure 11. Temperature dependence of the birefringence (δn), for FBA + 7BA complex in the nematic, smectic C, smectic F, and crystalline phases.

More over the plot of δn and temperature (Fig. 11) also acts as an additional proof for the different mesogenic transitions and their corresponding transition temperatures obtained earlier in the POM and DSC analysis. The determined order parameter S values plotted against temperature (Fig. 12) also evince the different transitions and their corresponding transition temperatures in FBA + 7BA mesogen under investigation.

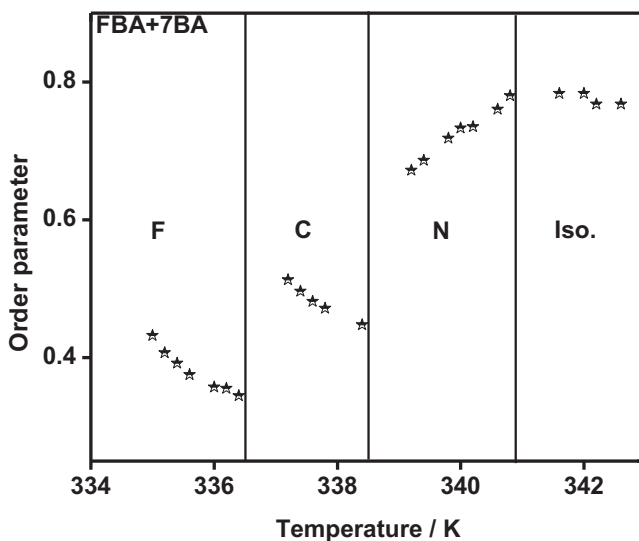


Figure 12. Temperature dependence of the order parameter S for FBA + 7BA complex.

5. Conclusions

- 1) A novel series of HBLC is synthesized and characterized by various techniques.
- 2) All the phases observed are confirmed by the textural observation and DSC studies.
- 3) The order of transition has been analyzed by Cox's parameter N_C .
- 4) Optical tilt angle for all the complexes in the smectic *C* phase is measured.
- 5) Order parameter evaluation through refractive measurement studies.

Acknowledgments

The infrastructural support rendered by Bannari Amman Institute of Technology and the financial support rendered by the Board of Research in Nuclear Sciences (BRNS) of Department of Atomic Energy (DAE), India (Sanction No. 2012/34/35/BRNS) are gratefully acknowledged by the authors.

References

- [1] Chandrasekhar, S. (1992). *Liquid Crystals*, Cambridge University Press: Cambridge, UK.
- [2] Marcel Dekker, F. D. (Ed.). (1979). *Liquid Crystals: The Fourth State of Matter*, Saeva: New York.
- [3] Paleos, C. M., & Tsiourvas, D. (2001). *Liq. Cryst.*, 28, 1127.
- [4] Paleos, C. M., & Tsiourvas, D. (1995). *Angew. Chem. Int. Ed. Engl.*, 34, 1696.
- [5] Kato, T. (1998). In: *Handbook of Liquid Crystals*, Vol. 2B, Demus, D., Goodby, J., Gray, G. W., Spiess, H. W., & Vill, V. (Eds.), Wiley-VCH: Weinheim, Chap. XVII.
- [6] Beginn, U., & Lattermann, G. (1994). *Mol. Cryst. Liq. Cryst.*, 241, 215.
- [7] Brienne, M. J., Gabard, J., Lehn, J. M., & Stibor, I. (1989). *J. Chem. Soc. Chem. Commun.*, 1868.
- [8] Kotera, M., Lehn, J. M., & Vigneron, J. P. (1994). *J. Chem. Soc. Chem. Commun.*, 197.
- [9] Willis, K., Price, D. J., Adams, H., Ungar, G., & Bruce, D. W. (1995). *J. Mater. Chem.*, 5, 2195.
- [10] Kihara, H., Kato, T., Uryu, T., Ujiie, S., Kumar, U., FreAchet, J. M. J., Bruce, D. W., & Price, D. J. (1996). *Liq. Cryst.*, 21, 25.
- [11] Willis, K., Luckhurst, J. E., Price, D. J., FreAchet, J. M. J., Kihara, H., Kato, T., Ungar, G., & Bruce, D. W. (1996). *Liq. Cryst.*, 21, 585.
- [12] Price, D. J., Willis, K., Richardson, T., Ungar, G., & Bruce, D. W. (1997). *J. Mater. Chem.*, 7, 883.
- [13] Yu, L. J., Wu, J. M., & Wu, S. L. (1991). *Mol. Cryst. Liq. Cryst.*, 198, 407.
- [14] Yu, L. J., & Pan, J. S. (1993). *Liq. Cryst.*, 14, 829.
- [15] Tsaih, J. J., & Yu, L. J. (1997). *Mol. Cryst. Liq. Cryst.*, 302, 339.
- [16] Bradfield, A. E., & Jones, B. (1929). *J. Chem. Soc.*, 2660.
- [17] Kato, T., & Frechet, J. M. J. (1989). *J. Am. Chem. Soc.*, 111, 8533.
- [18] Kumar, U., & Frechet Jean, M. J. (1992). *Adv. Mater.*, 4, 665.
- [19] Marthandappa, M., Somashekar, R., & Nagappa. (1991). *Phys. Status Solidi (a)*, 127, 259.
- [20] Saravanan, C., Deepa, M., Kannan, P., & Senthil, S. (2008). *Z. Naturforsch*, 63b, 571.
- [21] Trimper, S. (1987). *Phys. Status Solidi (a)*, 141, 369.
- [22] Yannopapas, V., Fytas, N., Kyrimi, V., Kallos, E., Vanakaras, A. G., & Photinos, D. J. (2013). *Phys. Status Solidi (a)*, 210, 335.
- [23] Thote, A. J., & Gupta, R. B. (2003). *Ind. Eng. Chem. Res.*, 42, 1129.
- [24] Li, J., Wisner, J. A., & Jennings, M. C. (2007). *Org. Lett.*, 9, 3267.
- [25] Paraschiv, I., Delforterie, P., Giesbers, M., Posthumus, M. A., Marcellis, A. T. M., Zuilhof, H., & Sudholter, E. J. R. (2005). *Liq. Cryst.*, 32, 977.
- [26] Kohlmeier, A., Nordsieck, A., & Janietz, D. (2009). *Chem. Mater.*, 21, 491.

- [27] Kato, T., Frechet, J. M. J., Wilson, P. G., Saito, T., Uryu, T., Fujishima, A., Jin, C., & Kaneuchi, F. (1993). *Chem. Mater.*, 5, 1094.
- [28] Kihara, H., Kato, T., Uryu, T., & Frechet, J. M. J. (1998). *Liq. Cryst.*, 24, 413.
- [29] Kato, T., Fujishima, A., & Frechet, J. M. J. (1990). *Chem. Lett.*, 919.
- [30] Kato, T., Wilson, P. G., Fujishima, A., & Frechet, J. M. J. (1990). *Chem. Lett.*, 19, 2003.
- [31] Kato, T., & Frechet, J. M. J. (1989). *Macromolecules*, 22, 3818.
- [32] Kumar, U., Kato, T., & Frechet, J. M. J. (1992). *J. Am. Chem.*, 114, 6630.
- [33] Kumar, U., Frechet, J. M. J., Kato, T., Ujiie, S., & Iimura, K. (1992). *Angew. Chem. Int. Ed. Engl.*, 31, 1531.
- [34] Kato, T., Mizoshita, N., & Kishimoto, K. (2006). *Angew. Int. Ed.*, 45, 38.
- [35] Gray, G. W., & Goodby, J. W. G. (1984). *Smectic Liquid Crystals: Textures and Structures*, Leonard Hill: London.
- [36] Shandryuk, G. A., Kuptsov, S. A., Shatalova, A. M., Plate, N. A., & Talroze, R. V. (2003). *Macromolecules*, 36, 3417.
- [37] Noot, C., Perkins, S. P., & Coles, H. J. (2000). *Ferroelectrics*, 244, 331.
- [38] Kavitha, C., Pongali Sathya Prabu, N., & Madhu Mohan, M. L. N. (2012). *Physica B*, 407, 859 and Kavitha, C., Pongali Sathya Prabu, N., & Madhu Mohan, M. L. N. (2013). *Mol. Cryst. Liq. Cryst.*, 574, 1, 96.
- [39] Kavitha, C., Pongali Sathya Prabu, N., & Madhu Mohan, M. L. N. (2012). *Phase Transitions*, 85, 973.
- [40] Kato, T., & Mizoshita, N. (2002). *Curr. Opin. Solid State Mater. Sci.*, 6, 579.
- [41] Kato, T., Uryu, T., Kaneuchi, F., Jin, C., & Frechet, J. M. J. (1993). *Liq. Cryst.*, 14, 1311.
- [42] Pavia, D. L., Lampman, G. M., & Kriz, G. S. (2007). *Introduction to Spectroscopy*, Sanat Printers: Kundli, India.
- [43] Nakamoto, K. (1978). *Infrared and Raman Spectra of Inorganic and Co-ordination Compounds*, Interscience: New York.
- [44] Kavitha, C., & Madhu Mohan, M. L. N. (2012). *J. Phys. Chem. Solids*, 73, 1203.
- [45] Xu, J. (2006). *J. Mater. Chem.*, 16, 3540.
- [46] Frechet, J. M. J., & Kato, T. (1992). *Hydrogen-bonded Liquid Crystal Complexes*. Patent US No. 5, 139, 696, dt. Aug.18.
- [47] Navard, P., & Cox, R. (1984). *Mol. Cryst. Liq. Cryst.*, 102, 261.
- [48] Priestly, E. B., Wojtowicz, P. J., & Sheng, P. (1975). *Introduction to Liquid Crystals*, Plenum Press: New York.
- [49] Stanley, H. E. (1971). *Introduction to Phase Transition and Critical Phenomena*, Clarendon Press: New York.
- [50] Loganathan, D. (2000). *Field cycling NMR studies of molecular dynamics in liquid crystals, Chapter 4. PhD thesis*, University of Hyderabad.
- [51] Kuczynski, W., Zywuicki, B., & Malecki, J. (2002). *Mol. Cryst. Liq. Cryst.*, 381, 1.
- [52] Balzarini, D. A. (1970). *Phys. Rev. Lett.*, 25, 914.
- [53] Haller, I., Huggins, H. A., & Freiser, M. J. (1972). *Mol. Cryst. Liq. Cryst.*, 16, 53.
- [54] de Gennes, P. G., & Prost, J. (1993). *The Physics of Liquid Crystals*, Oxford University Press: New York.